Experimental characterization of the heat transfer in internal flow for ethylene glycol-water mixtures

Rúben Alexandre Páscoa Ezequiel

ruben.ezequiel@tecnico.ulisboa.pt

Instituto Superior Técnico, Universidade de Lisboa, Portugal

January 2021

Keywords: Internal flow, Smooth Tube, Friction Factor, Heat transfer.

Abstract

The present work addresses the characterization of the flow, pressure drop and heat transfer in internal flow for a smooth tube, using distilled water and three water-ethylene glycol mixtures. The tube used has an internal diameter of 3,505 mm and a heat length of 2,4 m. Within this scope, an experimental setup was used, to perform and validate measurements of pressure drop and heat transfer in the laminar, transition and turbulent flow regimes. The Reynolds number varied approximately between 700 and 7000. The heat flux imposed on the tube wall varied between 0 kW/m^2 and 30 kW/m^2. The experimental results obtained for the friction factor and for the Nusselt number were validated for the laminar, transition and turbulent flow regimes, using available correlations in the literature. It was observed that the fluid that showed the lowest thermal losses, least friction factor, and best thermal performance factor in the laminar flow regime (relative to distilled water), was the 20% ethylene glycol and 80% water mixture. It was also observed that an increase in the heat flux applied triggered a delay in the transition of the flow. The fluid that presented the highest Nusselt number for high heat fluxes was the 50% ethylene glycol and 50% water mixture. The fluid that presented the highest j-Colburn factor for all the heat fluxes applied was the distilled water. Finally, the fluid that presented the best thermal performance factor in the turbulent flow regime (relative to distilled water) was the 50% ethylene glycol and 50% water mixture.

Introduction

Last generation heat exchangers (WCAC - Water charge air cooler), used in the intake circuit of internal combustion (IC) engine vehicles use cooling fluids instead of the incident air in the heat exchanger that promotes the heat exchange between two air circuits (ACAC – Air charge air cooler). The cooling fluid, ethylene glycol, is an integral and central part in guaranteeing the thermal efficiency of WCAC heat exchangers and is usually used in a mixture with water.

Ethylene glycol is used to reduce the melting point of water, since in colder countries, the ambient temperature can be below 0ºC. So, in order to prevent the freezing of the working fluid (which would lead the engine to overheat and be damaged), mixtures of water and ethylene glycol are used. The effect of ethylene glycol concentration in the water mixtures properties, and consequently the head loss and heat transfer mechanisms, is still poorly studied, and the water-ethylene glycol mixtures that are used are empirically selected.

This work consists in the study and experimental characterization of the head loss (friction factor), and heat transfer in internal flow in a smooth pipe for distilled water and ethylene glycol-water mixtures.

It is intended to evaluate the hydrodynamic behavior and the heat transfer processes, as a function of different relations of the ethylene glycol-water mixtures. This analysis includes the evaluation of different parameters such as the friction factor, Nusselt number, j-Colburn factor (among others), in a vast range of experimental conditions, in order to cover the three flow regimes (laminar, transition and turbulent). Distilled water will be used as the reference fluid. This study is justified by the fact that, as demonstrated in the context presented in previous paragraphs, there is still scarse information about the precise description of the thermal and hydrodynamic behavior of ethylene glycol when used in heat exchangers. On the other hand, empirically, companies like JDeus, which work on the development of heat exchangers for the automotive industry, have knowledge about the ethylene glycol deterioration after diverse use cycles, but don´t have detailed information on how that deterioration occurs and its effect on the flow and the heat transfer processes. The work developed here will essentially focus the effect of the percentage of ethylene glycol in the mixtures used, determining the range that allows the best hydrodynamic and thermal performance, so it can be used in diverse applications, namely the ones of interest for JDeus.

Experimental setup and procedures

Experimental setup

The experimental setup and all its components is represented in the following figure. The T and dP symbols refer, respectively, to the temperature and pressure sensors.

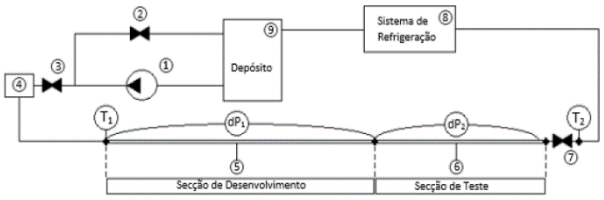

Figure 1: Schematic illustration of the experimental setup: (1) Hydraulic pump, (2) and (3) Valve, (4) Coriolis flow meter, (5) Development section, (6) Test section, (7) Spherical type valve with fine adjustment, (8) Mixing, heating and cooling system, (9) Filling deposit

In this experiment, a hydraulic pump (1) is used, through which the fluid pressure is raised, forcing it to flow through the experimental setup. The pump is connected to a frequency converter that allows to regulate the mass flow supplied in the setup. The valve (2) helps the flow regulation. So, when open, this valve forces a fraction of the flow to recirculate in the direction of the filling deposit (9), reducing the flow fraction that goes through the rest of the system. In this manner, as the valve (2) is closed, the flow fraction recirculated diminishes in the direction of the deposit and increases in the rest of the setup. Downstream of the pump, the fluid crosses a Coriolis flow meter (4), which measures the mass flow, the specific mass and the fluid temperature. Next, the fluid goes through the development section (5), composed of a stainless-steel steel AISI 304 tube, with a length of 0,65m and an internal diameter of 3,505mm. The length of the tube was defined in order to assure that the flow in its interior is hydrodynamically developed before entering the test section (6). The test section (6), represented in the following figure, is welded to the development section (5) and is composed of a stainless-steel AISI 304 tube, with a length of 2,4m and an internal diameter of 3,505mm.

In order to facilitate the welding process, it was chosen to use tubes with identical diameter sections, allowing a smoother connection between the development section (5) and the test section (6), consequently reducing the perturbations at the flow level caused by conventional hydraulic connections and diameter discontinuities. The test section (6) is heated by the Joule effect, being connected directly to a DC power source (HY5050EX of VOLTEQ), to assure a uniform heat flux in the tube surface (2,4m of length). The electrical power that is effectively applied in the tube surface is measured by a multimeter, connected to the entrance and exit of the test section (6), to account for the electrical power that is dissipated by the conducting cables.

Across the test tube surface, four type K thermocouples from Omega, were installed, with a distance between each one of approximately 600mm, allowing to determine the surface temperature in four distinct points. In addition, an addition two type K temperature sensors were installed: (T1) at the entrance of the development section (5) and (T2) at the exit of the test section (6). Problems were observed to occur in the measurements from the thermocouple at the exit of the test section. Therefore a semi open, fine cut valve (7) was installed, immediately before the sensor. This allows the valve (7) to operate as mixture chamber, promoting a better mixture of the fluid and, consequently, a more precise measurement of the average flow temperature at the sensor (T2) level.

To conclude, the fluid flows to a mixing, heating and cooling system (8), before returning to the hydraulic pump, completing the closed circuit.

Data treatment

The experimental data was processed following the procedure below:

Firstly, the properties of the fluid were evaluated, namely, the dynamic viscosity, μ, the specific heat, C_p, and the thermal conductivity, k, at the temperature $\bar{T}$:

$$\bar{T} = T_o + \frac{\Delta T}{2} \tag{1}$$

where T_o is the average temperature measured in the flow meter and $\Delta T = T_2 - T_1$.

In a tube, the Reynolds number is calculated using the following expression:

$$Re_D = \frac{4\dot{m}}{\pi D_h \mu} \tag{2}$$

where D_h represents the hydraulic diameter of the tube and $\dot{m}$ represents the mass flow rate. Since the tube is circular, $D_h \equiv D$.

The average fluid speed was also obtained:

$$u_m = \frac{4\dot{m}}{\rho \pi D_h^2} \tag{3}$$

where ρ represents the specific mass of the work fluid,

To obtain the friction factor, the following expression was used:

$$f = \frac{2D_h \Delta p}{\rho {u_m}^2 L} \tag{4}$$

where Δp represents the pressure drop across the tube and L the length between the two pressure sensors.

The Prandtl number Pr was obtained using the fluid properties through the expression below:

$$Pr = \frac{\mu C_p}{k} \tag{5}$$

The average thermal power, in watts [W], transferred to the work fluid was calculated by using the following expression:

$$\dot{q} = \dot{m} C_p \Delta T \quad (6)$$

An arithmetic average, given by the expression below, allowed to obtain the average temperature at the tube surface:

$$\bar{T}_s = \frac{t_1 + t_2 + t_3 + t_4}{4} \quad (7)$$

The average heat transfer coefficient was given by:

$$\bar{h} = \frac{\dot{m} C_p \Delta T}{\pi D_h L_{heated} (\bar{T}_s - \bar{T})} \quad (8)$$

where L_{heated} is the heated tube length. Therefore, it was possible to obtain the average Nusselt number $\overline{Nu}$:

$$\overline{Nu} = \frac{\bar{h} D_h}{k} \quad (9)$$

Next, the j-Colburn j was calculated:

$$j = \frac{Nu}{RePr^{1/3}} \quad (10)$$

The Grashof number Gr was also obtained:

$$Gr = \frac{g\beta(\bar{T}_s - \bar{T})D^3}{\nu^2} \quad (11)$$

where g represents the gravitational acceleration constant (9.81m/s^2) and β is the thermal expansion coefficient, evaluated at the temperature $\bar{T}$.

Finally, the Richardson's number Ri was also calculated:

$$Ri = \frac{Gr}{Re^2} \quad (12)$$

In this study, the relative error given in percentage was determined, using the following expression:

$$\%error = \frac{|V_m - V_p|}{V_p} \times 100 \quad (13)$$

where V_m simbolizes the measured value and V_p represents the predicted value, according to the literature. Therefore, the average relative error in percentage is given by:

$$\overline{\%error} = \frac{1}{N} \sum_{i=1}^{N} \frac{|V_{mi} - V_{pi}|}{V_{pi}} \times 100 \quad (14)$$

where N symbolizes the total number of points the sample studied.

Uncertainties

Table 1 shows the uncertainty of the physical properties used, coming from the literature and the from the specifications of the equipment used.

Table 1: Uncertainty of the physical properties used, coming from the literature and the from the specifications of the equipment used

Parameter	Uncertainty	Units
Temperature at the entrance of the development section, $\bar{T}_{in}$	$\pm 0{,}1$	[K]
Temperature at the exit of the test section, $\bar{T}_{out}$	$\pm 0{,}1$	[K]
Temperature difference between the entrance and exit, ΔT	$\pm 0{,}2$	[K]
Temperature of the tube surface, $\bar{T}_s$	$\pm 0{,}1$	[K]
Specific mass of the fluid, ρ	± 5	[kg/m^3]
Voltage, U	$\pm 0{,}015$	[V]
Current, I	$\pm 0{,}5$	[%]
Mass flow rate, $\dot{m}$	$\pm 0{,}2$	[%]

Results and Discussion

Description of the work conditions studied

For this work, 3 different ethylene glycol-water mixtures were selected, namely, (in volume) 20% ethylene glycol and 80% water, 35% ethylene glycol and 65% water, and 50% ethylene glycol and 50% water, to compare with the reference fluid, distilled water. The temperature at the entrance of the development section was kept constant, at around 25ºC. The experiments were performed for 3 different heat fluxes, 10, 20 and 30 kW/m^2, and then they were compared with the adiabatic conditions (without an applied heat flux), which were used as a reference for the validation of the experimental system. Since the dynamic viscosity varies from mixture to mixture, the necessary mass flows to obtain the same Reynolds numbers vary.

In the following table, the values of the most relevant thermophysical properties for the analysis performed here, evaluated at 25ºC are represented, to clarify the results descripted next.

Table 2: Values of thermophysical properties at 25ºC of the various fluids studied [12], [17], [20]

Thermophysical property	Distilled water	20% ethylene glycol and 80% water	35% ethylene glycol and 65% water	50% ethylene glycol and 50% water
Density, ρ [kg/m³]	997	1028	1052	1076
Prandtl number, Pr	6.13	13*	16*	30*
Dynamic viscosity, μ [Pa*s]	0.00089	0,00146	0,00258	0,00309
Specific heat, C_p [J/Kg*K]	4138	3958	3675	3402

* Approximated values.

Thermal losses analysis

As previously stated, in this work, a heat source of direct current was used, and so, it was possible to apply a constant heat flux in the tube wall, used experimentally. Therefore, the thermal power imposed in the tube wall is given by the following expression:

$$q_{imp} = UI \tag{15}$$

Where U represents the voltage and I the current supplied by the power supply.
Since there are thermal losses to the environment, in reality, the thermal power effectively transferred to the fluid was determined using the following expression:

$$q_{efet} = \dot{m} C_p (T_{in} - T_{out}) \tag{16}$$

Where $\dot{m}$ is the mass flow rate of the fluid circulating inside the tube and C_p is the specific heat, evaluated at the temperature transferred between T_{in} and T_{out}. From With these quantities, it is possible to define a dimensionless parameter, called thermal efficiency η. It is calculated using the following expression:

$$\eta = \frac{q_{efet}}{q_{imp}} \tag{17}$$

From the thermal efficiency, it is also possible to define another parameter, P_{term}, that represents the thermal losses, in percentage. It is calculated using the following expression:

$$P_{term} = (1 - \eta) * 100 \tag{18}$$

Firstly, it was verified that, in general, the thermal losses are approximately inversely proportional to the Reynolds number, decreasing as the Reynolds number increases (although there were exceptions, due to errors in the measurement). Comparing the results for each applied heat fluxes, the thermal losses for the mixtures remained approximately constant, except for the distilled water, for which, as the heat flux increased, the thermal losses decreased. It was also observed that, for a sufficiently high Reynolds number (around 3000), the thermal losses became negative in several cases. This can be explained by the fact that the turbulence generated in turbulent flow increases the mixing capacity and the flow becomes more chaotic, leading to temperature fluctuations. The largest registered value of a thermal loss was 11,90%, whereas the smallest value was -12,75%, therefore, it is possible to conclude that the heat exchange was efficient.

These experiments allowed to conclude that the heat exchange is more efficient (fewer thermal losses) in the turbulent flow regime than in the laminar flow regime, and as so, when it is important to optimize the energy consumption, this is an important factor to consider.

For the applied heat flux of 10kW/m², the mixture that had the best performance was the 20% ethylene glycol and 80% water, with an average thermal loss of 2,38%. For the applied heat flux of 20kW/m², the mixture that had the best performance was the 20% ethylene glycol and 80% water, with an average thermal loss of 4,39%. For the applied heat flux of 30kW/m², the mixture that had the best performance was the 20% ethylene glycol and 80% water, with an average thermal loss of 3,5%. The results allow to conclude that the mixture that had the fewer thermal losses was the 20% ethylene glycol and 80% water.

Friction factor analysis

Firstly, the experiments were performed in adiabatic conditions (without an applied heat flux). The first fluid tested was distilled water, to work as the base reference to study the mixtures. The results are represented in the following figure, where it is expressed the friction factor obtained experimentally, as a function of the Reynolds number. The curves of the friction factor coming from the revised correlations in the literature are also showed, for the various flow regimes.

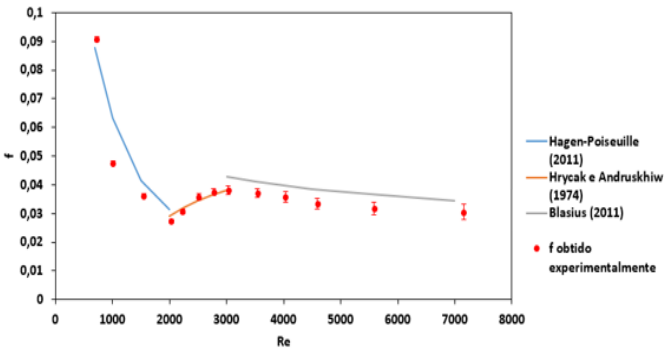

Figure 2: Friction factor as a function of the Reynolds number for distilled water without an applied heat flux (the error bars represent the calculated associated uncertainty)

The following table shows the absolute average and absolute maximum deviations of the previous experimental results in relation to the expected theoretical values from the empirical correlations of the literature.

Table 3: Absolute average and absolute maximum deviations that the experimental results present in relation to different literature correlations

Regime	Correlation	Absolute average deviation (%)	Absolute maximum deviation (%)
Laminar	Hagen-Poiseuille (2011)	13,67	24,97
Transition	Hrycak e Andruskhiw (1974)	3,36	6,28
Turbulent	Blasius (2011)	11,41	13,39

Table 3 shows that the deviations between the correlations and the experimental data were not significative.

For the laminar flow regime, the experimental results were quite close to the expected values through the Hagen-Poiseuille correlation (2011), having an absolute average deviation of 13,67%.

For the transition regime, the experimental results came really close to the expected values through the Hrycak and Andruskhiw correlation (1974), having an absolute average deviation of only 3,36%.

For the turbulent regime, the experimental results were close to the expected values through the Blasius correlation (2011), having an absolute average deviation of 11,41%.

After obtaining the results for distilled water, the friction factor was analyzed for the three ethylene glycol-water mixtures used. The results are showed in the following figure.

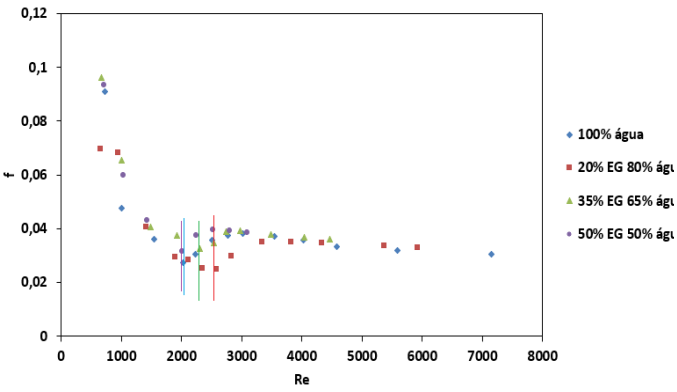

Figure 3: Friction factor as a function of the Reynolds number for the various fluids analyzed without an applied heat flux (vertical lines represent the start of transition for each fluid respectively)

Firstly, it is possible to conclude that the transition from laminar to the turbulent flow regime occurs sooner for the distilled water (at around Re = 2000), followed by the 50% ethylene glycol and 50% water mixture, followed by the 35% ethylene glycol and 65% water mixture, and finally, followed by the 20% ethylene glycol and 80% water mixture, starting around $Re = 2700$. This can be explained by the fact that the increase in viscosity due to the presence of ethylene glycol (much more viscous than water) causes some of the perturbations that induce transition to be attenuated, delaying the transition for the ethylene glycol-water mixtures. The delay in the transition does not depend directly on the amount of ethylene glycol in the mixture, it is more related to the perturbations that can be induced in the flow.

It can be observed that the friction factor is generally higher for the 50% ethylene glycol and 50% water mixture, and smaller for the 20% ethylene glycol and 80% water mixture. However, for higher Reynolds numbers (above 4500), distilled water eventually presents the lowest friction factor, since its low viscosity causes the head losses (and consequently the friction factor) to remain small in relation to the mixtures. In theory, the friction factor in adiabatic conditions should be inferior for the distilled water, since its viscosity is inferior to the other fluids. This was not verified due to errors in data acquisition and due to impurities that existed in the system.

Experiments were also performed in diabatic conditions (with an applied heat flux), namely for 10, 20 and 30 kW/m^2 heat fluxes.

The results are clear for the applied heat flux of 30 kW/m^2 as shown below. These results are consistent with those obtained for the applied heat fluxes of 10 and 20 kW/m^2 which are not presented here due to paper length constrictions.

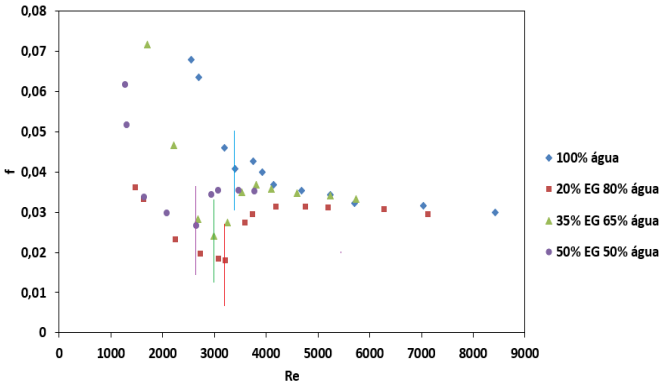

Figure 4: Friction factor as a function of the Reynolds number for the 30 kW/m^2 applied heat flux, for the various fluids studied (vertical lines represent the start of transition for each fluid respectively)

From the previous figure, it can be observed that the transition from laminar to turbulent flow regimes occurs sooner, i.e for lower values of the Reynolds number, for the 50% ethylene glycol and 50% water mixture, starting at Re=2800, followed by the 35% ethylene glycol and 65% water mixture, followed by the 20% ethylene glycol and 80% water mixture, and lastly, followed by the distilled water, starting at around Re=3500.

It can also be observed that the friction factor is, in general, inferior for the 20% ethylene glycol and 80% water mixture.

It can be concluded that, for both adiabatic and diabatic conditions, the fluid that showed the smaller friction factor was obtained for the 20% ethylene glycol and 80% water mixture. This is due to the fact that its viscosity is the lowest when compared to the other mixtures. However, for sufficiently high Reynolds

numbers (above 5000), the distilled water eventually presents the lowest friction factor due to its low viscosity when compared with the other fluids. The water does not present a lower friction factor for lower Reynolds numbers for the reason that is explained in the next paragraph.

For higher heat fluxes, the fluid for which the transition occurs later is the distilled water, in contrast to what was verified in adiabatic conditions. This is due to the fact that this fluid presented the highest temperature difference between the entrance and exit (because the flow rate was always inferior in relation to the other fluids), for any Reynolds number. This caused the dynamic viscosity to be inferior (since it decreases with temperature increase), as it's calculated at the average temperature between the entrance and exit. This caused the Reynolds range where transition happened to be a lot higher than the other fluids, causing the friction factor to remain higher for a larger Reynolds range.

Convection analysis

The Richardson's number was calculated, in order to determine which convection type was dominant in the experiments. The following figures depict the results obtained for the various fluids.

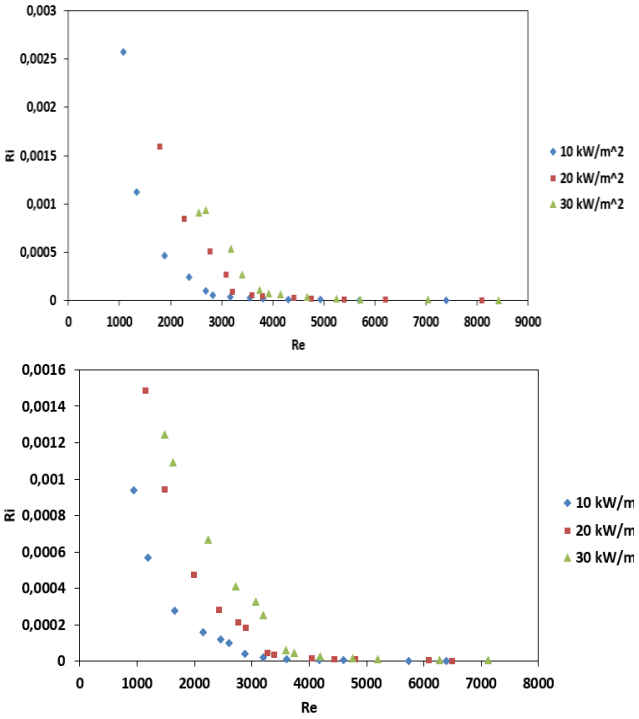

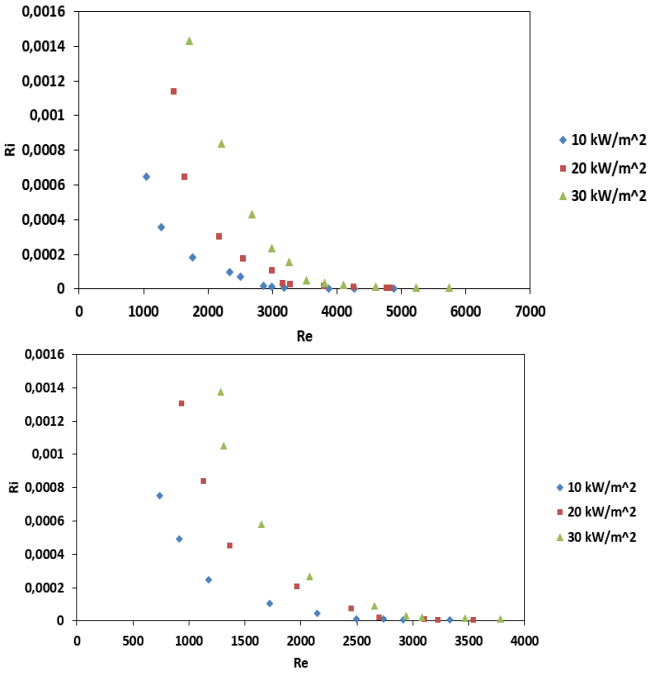

Figures 5, 6, 7 and 8: Richardson's number as a function of the Reynolds number for the distilled water, 20% ethylene glycol and 80% water, 35% ethylene glycol and 65% water and 50% ethylene glycol and 50% water mixtures respectively, for the various heat fluxes applied

From the previous figures, it can be observed that the Richardson's number is always lower than 0,1.

Hence, it is possible to conclude that the natural convection can be ignored and there is mostly only forced convection.

Analysis of the heat transfer processes

This analysis is made in two parts: firstly, an assessment is done to each mixture, comparing the results obtained for each heat flux studied. In the second part, for each heat flux, the results for each fluid are compared for the various mixtures.

To start, the experiments for distilled water were made, with the goal of having a base of reference or the later experiments. The results are expressed in the following figure.

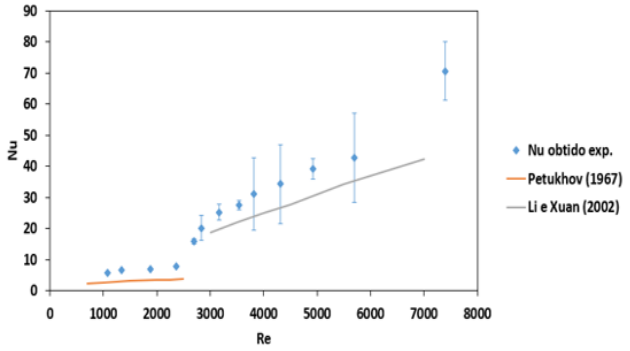

Figure 9: Nusselt number as a function of the Reynolds number for distilled water with an applied heat flux of 10kW/m^2 (the error bars represent the calculated associated uncertainty)

The following table shows the absolute average and absolute maximum deviations of the previous experimental results in relation to the expected theoretical values from the empirical correlations of the literature.

Table 4: Absolute average and absolute maximum deviations that the experimental results present in relation to different literature correlations

Regime	Correlation	Absolute average deviation (%)	Absolute maximum deviation (%)
Laminar	Petukhov (1967)	105,41	114,35
Turbulent	Li and Xuan (2002)	20,28	35,47

Table 4 shows that the deviations between the experimental data and the theoretical correlations were substantial for the laminar flow regime. Hence, the experimental results were quite different from the expected values through the Petukhov correlation (1967), having an absolute average deviation of 105,41%. This was possibly due to perturbations induced in the flow and errors in the data acquisition. It is also possible that the correlation is not adequate for the experimental conditions covered here using ethylene glycol. Although the error is large, the scale of the Nusselt number is always inferior to 10 in the laminar flow regime.

For the turbulent flow regime, the experimental results were relatively close to the expected values through the Li and Xuan correlation (2002), having an absolute average deviation of 20,28%.

From this analysis it is possible to conclude that the Nusselt number variation had the expected behavior, being much higher in the turbulent regime than in the laminar regime. However, the experimental values were underestimated by the Li and Xuan (2002) correlation. This can be explained due to errors and uncertainties in the measurement, and due to impurities, that were in the system. These results were used as the base of reference for the experiments that follow next.

After obtaining the results for distilled water, the Nusselt number was analyzed for the three ethylene glycol-water mixtures used. The results are showed in the following figures.

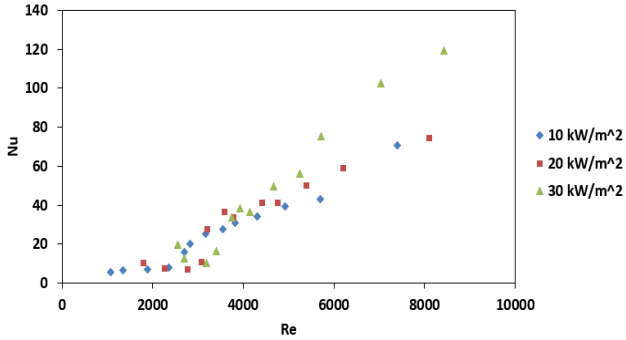

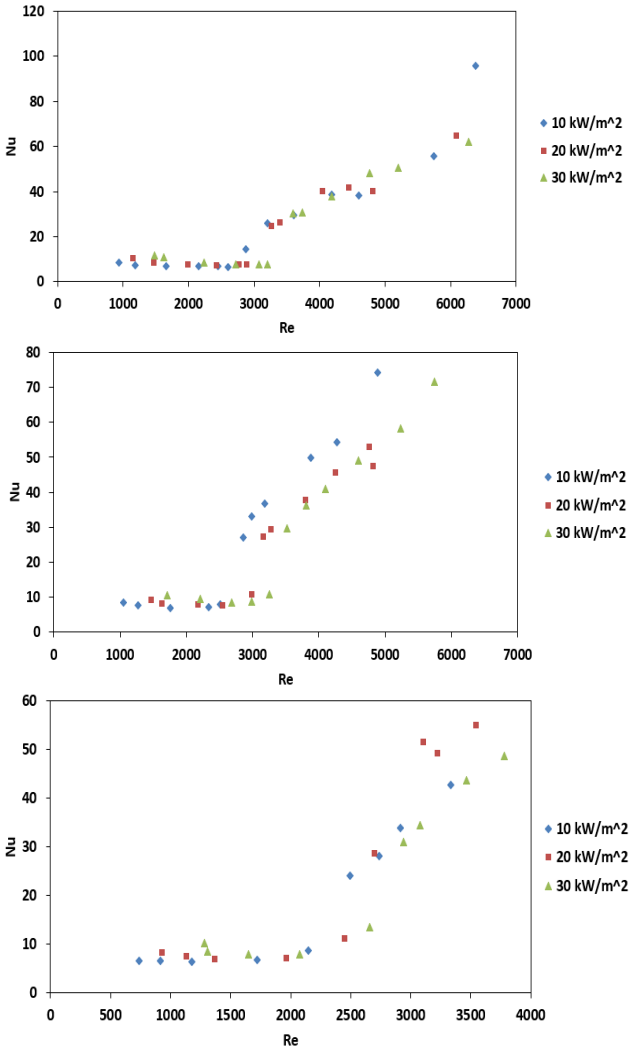

Figures 10, 11, 12 and 13: Nusselt number as a function of the Reynolds number for the distilled water, 20% ethylene glycol and 80% water, 35% ethylene glycol and 65% water and 50% ethylene glycol and 50% water mixtures respectively, for the various heat fluxes applied

From these results, it is possible to conclude that, in general, an increase in the applied heat flux causes the transition from the laminar to the turbulent flow regime to be delayed, i.e. to occur at higher Reynolds numbers, but the effect in the Nusselt number itself varies from case to case. This can be explained by the viscosity reduction as a function of the temperature, increasing the Reynolds number, overlapping the dampening effects caused by the viscosity increase as the amount of ethylene glycol in the mixture increases.

In the second part of the analysis, for each heat flux, the results for each fluid are compared, as depicted in the following figures.

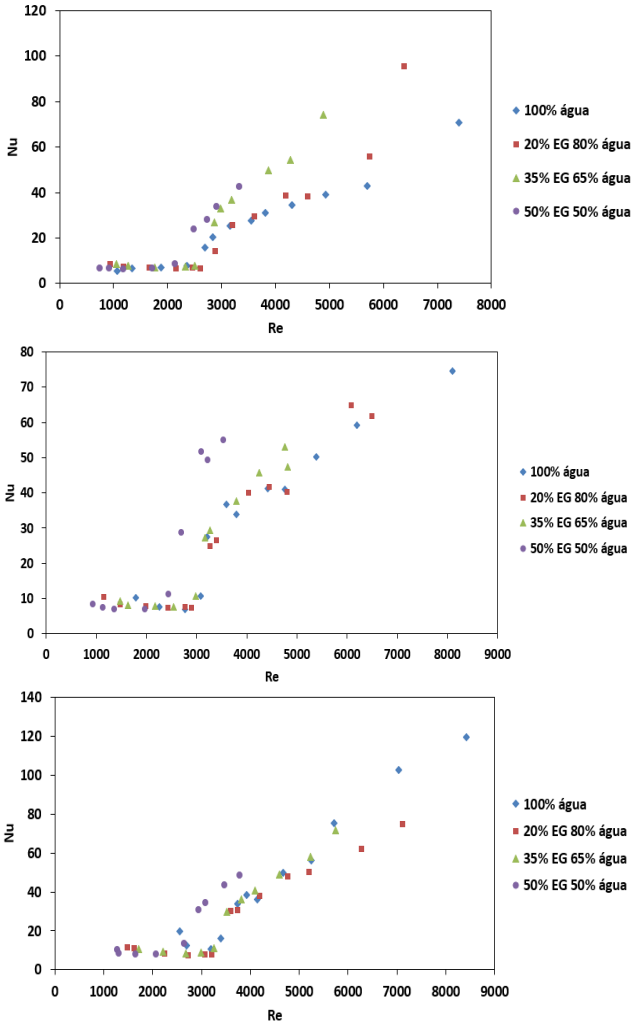

Figures 14, 15 and 16: Nusselt number as a function of the Reynolds number for the 10, 20 and 30 kW/m^2 heat fluxes applied respectively, for the various fluids studied

It can be observed that, as the heat flux increases, the transition of the flow is progressively more delayed, as it was verified in the previous analysis.

From these results, it is possible to conclude that, in general, for high applied heat fluxes, the fluid that presents the higher Nusselt number is the 50% ethylene glycol and 50% water mixture.

<u>j-Colburn factor analysis</u>

The following figure presents the results obtained for the 30 kW/m^2 applied heat flux. The results for the 10 and 20 kW/m^2 applied heat fluxes are in the full dissertation of this work.

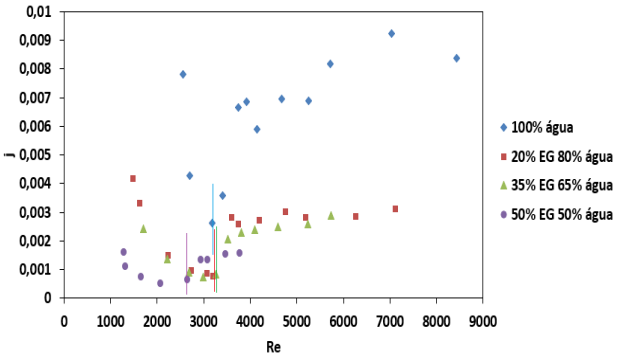

Figure 17: j-Colburn factor as a function of the Reynolds number for the 30 kW/m^2 applied heat flux, for the various fluids studied (vertical lines represent the start of transition for each fluid respectively)

From these results, it is possible to conclude that, in general, the behavior of the j-Colburn factor and friction factor curves are very similar.

It can be observed that the fluid that had, in general, the highest j-Colburn factor, is the distilled water. However, the friction factor measured was not as low as the one measured for the 20% ethylene glycol and 80% water mixture. Using this mixture instead, the optimal zone of work for a heat exchanger would be for $Re \approx 3300$, where the friction factor is minimum and j-Colburn factor is high.

From this analysis, it can be concluded that the fluid that had the best thermal performance (higher j-Colburn factor) is the distilled water. However, if the objective is to minimize the friction factor, the mixture to be used is the 20% ethylene glycol and 80% water.

A helpful parameter to evaluate the flow transition is the j-Colburn factor derivative. The following figures show the results obtained for the various fluids studied, for the various heat fluxes studied.

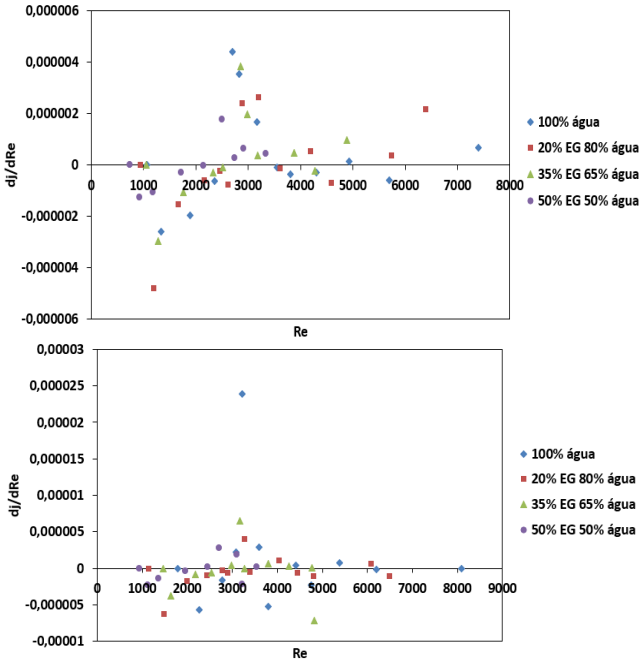

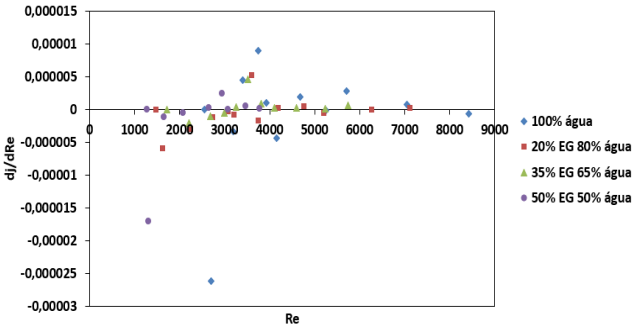

Figures 18, 19 and 20: j-Colburn factor derivative, as a function of the Reynolds number, for the 10, 20 and 30 kW/m^2 heat fluxes applied respectively, for the various ethylene glycol-water mixtures studied

The point of transition is located in the first signal change of the j-Colburn factor derivative, from negative to positive.

The previous figures allow to confirm the location of the points of the beginning of the transition described previously in the friction factor analysis (in diabatic conditions).

Another interesting parameter to evaluate is the thermal performance of a fluid (in this case, relative to distilled water), is the thermal performance factor. The following figures show the results obtained for the three ethylene glycol-water mixtures, as a function of the Reynolds number, for the various heat fluxes studied.

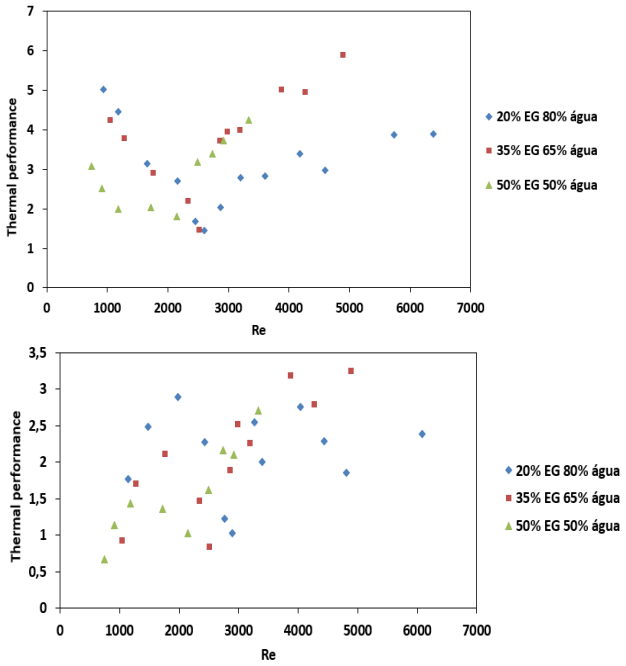

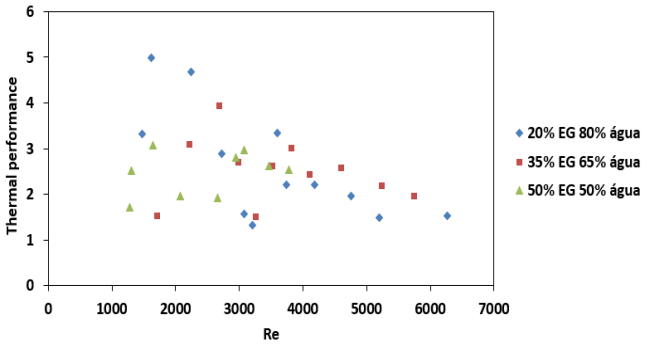

Figures 21, 22 and 23: Thermal performance factor, as a function of the Reynolds number, for the 10, 20 and 30 kW/m^2 heat fluxes applied respectively, for the various ethylene glycol-water mixtures studied

From these results, it is possible to conclude that, for the laminar regime, the mixture that presented the best thermal performance factor was the 20% ethylene glycol and 80% water mixture. This is due to the fact that, based on the previous analysis, it was observed that this mixture had the smallest friction factor in the laminar regime, in comparison with the other mixtures. If we are developing a heat exchanger to work in this regime, this should be the mixture used.

In many cases, it can be observed that there is an abrupt increase in the thermal performance factor, for the fluids used, for $Re \sim 3000$. This corresponds to the transition region, where there is a big increase of the Nusselt number and small increase in the friction factor. Since the increase, in percentage, of the Nusselt number is a lot higher than the friction factor, the thermal performance factor increases.

In the turbulent regime, it is possible to notice that the fluid that presents the best thermal performance factor is the 50% ethylene glycol and 50% water mixture. So, it can be concluded that this mixture is the one that presents the best thermal performance in the turbulent regime. However, the friction factor is higher for this fluid, so if we are designing a heat exchanger in this regime that uses this mixture, this should be taken into account.

Conclusions

The fluid that showed the lowest thermal losses, least friction factor, and best thermal performance in the laminar flow regime (relative to distilled water), was the 20% ethylene glycol and 80% water mixture. It was also observed that an increase in the heat flux applied provoked a delay in the transition of the flow. The fluid that presented the highest Nusselt number for high heat fluxes was the 50% ethylene glycol and 50% water mixture. The fluid that presented the highest j-Colburn factor for every heat flux applied was the distilled water. Finally, the fluid that presented the best thermal performance in the turbulent flow regime (relative to distilled water) was the 50% ethylene glycol and 50% water mixture.

Nomenclature

A_s	Surface area of the tube (m^2)
D	Internal tube diameter (m)
f	Friction factor
Gr	Grashof's number
h	Heat transfer coefficient (W/m^2*K)
I	Current intensity (A)
j	j-Colburn factor
k	Thermal conductivity ($W*m^{-1}*K^{-1}$)
L	Tube length (m)
$\dot{m}$	mass flow rate (kg/s)
Nu	Nusselt number
P_{term}	Thermal loss (in percentage)
Pr	Prandtl number
q_{efet}	Effective thermal power transferred to the fluid [W]
q_{imp}	Imposed thermal power on the tube wall [W]
q''	Heat flux (W/m^2)
R_e	Reynolds number
Ri	Richardson's number
t	Time (s)
T	Temperature (ºC/K)
U	Voltage [V]
x	Axial position in the tube (mm)
δ	Hydrodynamic/Thermal boundary layer thickness (mm)
ΔT	Temperature gradient (ºC/K)
η	Thermal efficiency
μ	Dynamic viscosity [Pa*s]
ρ	Specific mass [kg/m^3]

Acknowledgments

The author acknowledges IN+ for the opportunity to do this work, to professor Ana Moita for all the support and guidance offered during the entire time, for the excellent work environment provided by his colleagues and to Instituto Superior Técnico for the excellence of the knowledge transmitted through the years of the course.

References

[1] Incropera, F. P., DeWitt, D. P., Bergman, T. L., & Lavine, A. S., (2011). Fundamentos de Transferência de Calor e de Massa. Rio de Janeiro: John Wiley & Sons.

[2] Everts, M., & Meyer, J. P. (2017). Heat transfer of developing and fully developed flow in smooth horizontal tubes in the transitional flow regime. International Journal of Heat and Mass Transfer, 117, 1331-1351.

[3] Andrade, F. (2018). Caracterização Experimental da Transmissão de Calor em Escoamentos no Interior de Tubos Corrugados. Dissertação de Mestrado em Engenharia Mecânica. Lisboa: Instituto Superior Técnico.

[4] Cautela, R. (2019). Descrição dos mecanismos de ebulição em meio quiescente usando superfícies bifílicas. Dissertação de Mestrado em Engenharia Mecânica. Lisboa: Instituto Superior Técnico.

[5] Ghajar, A. J., & Tam, L. M. (1994). Heat transfer measurements and correlations in the transition region for a circular tube with three different inlet configurations. Experimental thermal and fluid science, 8(1), 79-90.

[6] Tam, H. K., Tam, L. M., & Ghajar, A. J. (2012). Effect of inlet geometries and heating on the entrance and fully-developed friction factors in the laminar and transition regions of a horizontal tube. Experimental Thermal and Fluid Science, 44, 680–696.

[7] Andrade, F., Moita, A. S., Nikulin, A., Moreira, A. L. N., Santos, H. (2019). Experimental investigation on heat transfer and pressure drop of internal flow in corrugated tubes. International Journal of Heat and Mass Transfer, 140, 940–955.

[8] Everts, M., & Meyer, J. P. (2015). Heat transfer characteristics of developing flow in the transitional flow regime of a solar receiver tube. Presented at the 3rd Southern African Solar Energy Conference, South Africa.205.

[9] Romeo, E., Royo, C., & Monzón, A. (2001). Improved explicit equations for estimation of the friction factor in rough and smooth pipes. Chemical Engineering Journal, 86, 369–374.

[10] Promvonge, P., & Thianpong, C. (2008). Thermal performance assessment of turbulent channel flows over different shaped ribs. International Communications in Heat and Mass Transfer, 35, 1327–1334.

[11] Taylor, B. N., & Kuyatt, C. E. (1994). Guidelines for Evaluating and Expressing the Uncertainty of NIST Measurement Results. NIST Technical Note, 1297, 20.

[12] Bohne, D., Fischer, S., & Obermeier, E. (1984). Thermal conductivity, Density, Viscosity, and Prandtl-Numbers of Ethylene Glycol-Water Mixtures. Ber. Bunsenges. Phys. Chem. 88, 739-742.

[13] Tam, L. M., & Ghajar, A. J. (1997). Effect of Inlet Geometry and Heating on the Fully Developed Friction Factor in the Transition Region of a Horizontal Tube. Experimental Thermal and Fluid Science, 15(1), 52–64.

[14] Nikulin, A., Moita, A. S,. Moreira, A. L. N., Murshed, S. M. S., Huminic, A., Grosu, Y., Faik, A., Nieto-Maestre, J., & Khliyeva, O. (2018). Effect of Al2O3 nanoparticles on laminar, transient and turbulent flow of isopropyl alcohol. International Journal of Heat and Mass Transfer, 130, 1032–1044.

[15] Fang, X., Xu, Y., & Zhou, Z. (2010). New correlations of single-phase friction factor for turbulent pipe flow and evaluation of existing single-phase friction factor correlations. Nuclear Engineering and Design, 241, 897–902.

[16] Brederode, V. (2014). Aerodinâmica Incompressível: Fundamentos. Lisboa, Portugal: IST Press.

[17] Yue, H., Zhao, Y., Ma, X., & Gong, J. (2011). Ethylene glycol: properties, synthesis, and applications. Chemical Society Reviews, 41, 4218–4244.